Construction of Bis-pyrazole Based Co(II) Metal–Organic Frameworks and Exploration of Their Chirality and Magnetic Properties

ARTICLE *in* CRYSTAL GROWTH & DESIGN · MAY 2014

Impact Factor: 4.89 · DOI: 10.1021/cg500174g

8 AUTHORS, INCLUDING:

Arijit Goswami
Indian Association for the Cultivation of Science
13 PUBLICATIONS **134** CITATIONS
SEE PROFILE

Bappaditya Gole
Indian Institute of Science
24 PUBLICATIONS **648** CITATIONS
SEE PROFILE

Sumi Ganguly
Indian Association for the Cultivation of Science
9 PUBLICATIONS **84** CITATIONS
SEE PROFILE

Sumit Khanra
Indian Institute of Science Education and Res…
36 PUBLICATIONS **624** CITATIONS
SEE PROFILE

CRYSTAL GROWTH & DESIGN

Article

pubs.acs.org/crystal

Construction of Bis-pyrazole Based Co(II) Metal–Organic Frameworks and Exploration of Their Chirality and Magnetic Properties

Sudeshna Bhattacharya,[†] Arijit Goswami,[†] Bappaditya Gole,[‡] Sumi Ganguly,[†] Sukhen Bala,[†] Satirtha Sengupta,[†] Sumit Khanra,[§] and Raju Mondal*[,†]

[†]Department of Inorganic Chemistry, Indian Association for the Cultivation of Science, Raja S. C. Mullick Road, Kolkata 700032, West Bengal, India

[‡]Department of Inorganic and Physical Chemistry, Indian Institute of Science, Bangalore 560 012, India

[§]Department of Chemical Sciences, Indian Institute of Science Education and Research, Kolkata, Mohanpur, West Bengal 741252, India

Supporting Information

ABSTRACT: In continuation of our interest in pyrazole based multifunctional metal–organic frameworks (MOFs), we report herein the construction of a series of Co(II) MOFs using a bis-pyrazole ligand and various benzene polycarboxylic acids. Employment of different acids has resulted in different architectures ranging from a two-dimensional grid network, porous nanochannels with interesting double helical features such as supramolecular chicken wire, to three-dimensional diamondoid networks. One of the distinguishing features of the network is their larger dimensions which can be directly linked to a relatively larger size of the ligand molecule. Conformational flexibility of the ligand also plays a decisive role in determining both the dimensionality and topology of the final structure. Furthermore, chirality associated with helical networks and magnetic properties of two MOFs have also been investigated.

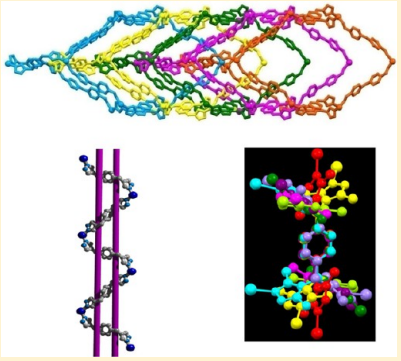

INTRODUCTION

The last two decades have witnessed a tremendous growth in the field of metal–organic frameworks (MOFs) owing to their diverse potential applications, ranging from gas sorption and storage, magnetism, catalysis to biomedical utilities.[1] Such potential bulk properties of MOFs are often found to be intimately related to the network topology and dimensionalities.[2] One such topology related property would be chirality of the framework. It has been observed that, even in absence of any chiral ligand, chirality in a network can be induced via spontaneous resolution.[20] The resultant chiral MOFs can be of great importance in the fields of chiral heterogeneous catalysis and chiral separation.

The structural modularity, on the other hand, depends heavily on the appropriate combination of metal centers, coordinating functional groups, and the geometry of the predesigned ligands.[3] Accordingly, ligand molecules with various functional groups, with different conformations and spacers between the coordinating sites, have been extensively used.[4] However, one can hardly overlook the overwhelming usage of pyridyl and carboxylate as coordinating functional groups, despite their serious shortcomings toward functional materials.[5] For example, MOFs made of neutral pyridyl-based linkers frequently end up with a structure where non-coordinated anions occupy the channels of the frameworks, reducing the porosity in the framework.[6] This is exactly where relatively less explored azole based ligands are really handy. It has been observed that polyazole bridging ligands with strong metal–nitrogen bonds provide remarkably strong chemical and thermal stability and lead to a slow but steady shift in favor of azole based MOFs synthesis.[7]

Notwithstanding of their strong presence in traditional coordination complex synthesis, 1H-pyrazole based ligands especially containing a flexible backbone are seldom reported in the literature.[8] This is particularly true for magnetic polymeric networks, one of the most studied branch of MOFs.[9] In particular, the relationship between the structural aspects of MOFs and magnetic properties has attracted extensive attention in recent times with the aim of understanding the fundamental factors governing magnetic properties. Despite a plethora of recent literature sources on magnetic MOFs, such networks based on 1H-pyrazole based ligands still remain one of the most intriguing yet elusive varieties.[10] Notwithstanding, pyrazole based ligands offer a broad scope of study of magnetic MOFs.

Flexibility of the ligands is another interesting and key issue, yet often overlooked during MOF synthesis.[11] A rigid ligand almost invariably leads to an inflexible framework. On the

Received: January 31, 2014
Revised: May 5, 2014
Published: May 7, 2014

   dx.doi.org/10.1021/cg500174g | *Cryst. Growth Des.* 2014, 14, 2853–2865

Scheme 1

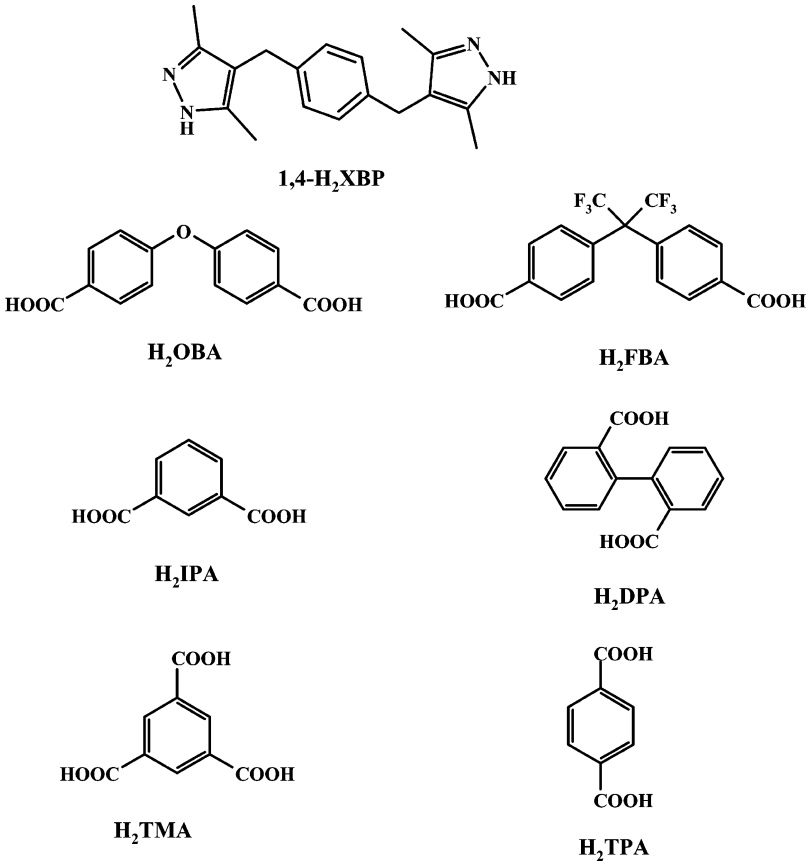

contrary, there is an increasing recognition that incorporation of a degree of flexibility in the network may yield some advantages by enhancing its reversible response to the presence or absence of guests.[12] One of the popular ways of introducing flexibility in the network is to incorporate a flexible bridging ligand.[13] The ability of flexible ligands to adopt, depending on the coordination requirement, different conformations via bending, stretching, twisting, or rotating when coordinating to the metal center remains the major driving force behind this trend.[14]

Our recent work on the design and synthesis of functional nanoporous MOFs is highly relevant in this regard.[15] We have demonstrated the usefulness of pyrazole based bridging ligands in multifunctional MOF synthesis, especially in a mixed ligand system with the formation of a characteristic hydrogen bonded motif with the monodentate carboxylate group (Scheme 1). Furthermore, the flexible core present in these pyrazole based ligands led to a wide range of conformations which have often turned out to be the structure determining factor by exerting considerable structural influence to form diverse topologies.

Inspired by the aforesaid facts, we now extend our work along these lines by employing another flexible bispyrazole based ligand, 4-(4-((3,5-dimethyl-1*H*-pyrazol-4-yl)methyl)-benzyl)-3,5-dimethyl-1*H*-pyrazole (H_2XBP) (Scheme 1). The H_2XBP molecule has flexible methylene groups between the pyrazole rings and the central benzene ring, which makes the ligand have flexible conformations and better adaptability. At the same time this enhances the possibility of various self-assembly and topologies for resultant polymeric networks. The flexibility also arises from the nearly unhindered torsion of the pyrazole rings along the single bond between the rings and can lead to different conformations.

Moreover, the presence of in-built hydrogen bonding sites, a special characteristic feature of 1-H pyrazole rings, makes it another interesting system for supramolecular self-assembly study. Our previous work demonstrated that the non-coordinating protonated nitrogen atom of the pyrazole moiety normally acts as a donor atom in hydrogen bonds and often plays a pivotal role in a mixed ligand system containing aromatic polycarboxylates (Scheme 1).[13]

In continuation to our interest in pyrazole based ligand molecules, we explore the synthesis of MOFs in a mixed ligand system using H_2XBP and various benzene polycarboxylic acids. In this contribution, we report the synthesis and structural aspects of seven MOFs, $\{[Co(H_2XBP)(TPA)]\cdot(H_2O)_{0.5}\}_n$ (**1**), $\{[Co(H_2XBP)(IPA)]\cdot(H_2O)(CH_3OH)\}_n$ (**2**), $\{[Co(H_2XBP)(DPA)]\cdot(H_2O)\}_n$ (**3**), $[Co(H_2XBP)_{0.5}(FBA)]_n$ (**4**), $\{[Co_2(H_2XBP)_2(OBA)_2]\cdot(H_2O)_{0.5}\}_n$ (**5**), $\{Co_2(H_2XBP)(TMA)_2(H_2O)](CH_3OH)\}_n$ (**6**), $\{Co(H_2XBP)_{0.5}(HTMA)(CH_3OH)]_n$ (**7**) {where, H_2TPA = terephthalic acid, H_2IPA = isophthalic acid, H_2OBA = 4,4′-oxybis (benzoic acid), H_2FBA = 4,4′-(hexafluoroisopropylidene)bis(benzoic acid), H_2TMA = trimesic acid, H_2DPA = dipehnic acid } obtained from cobalt-nitrate and respective mixed ligand systems by means of solvothermal techniques. Furthermore, magnetic properties of compounds **4** and **7** have also been investigated.

EXPERIMENTAL SECTION

Materials and General Method. H_2XBP was synthesized by a published procedure.[16] All reagents and chemicals were purchased from commercial sources and were used without further purification.

dx.doi.org/10.1021/cg500174g | *Cryst. Growth Des.* 2014, 14, 2853−2865

Table 1. Crystallographic Data and Refinement Parameters for Compounds 1−7

	1	2	3	4	5	6	7
empirical formula	$C_{52}H_{54}Co_2N_8O_9$	$C_{54}H_{58}Co_2N_8O_{11}$	$C_{32}H_{32}CoN_4O_5$	$C_{26}H_{19}CoF_6N_2O_4$	$C_{128}H_{122}Co_4N_{16}O_{21}$	$C_{148}H_{144}Co_8N_{16}O_{60}$	$C_{19}H_{19}CoN_2O_7$
crystal system	monoclinic	monoclinic	triclinic	monoclinic	orthorhombic	monoclinic	triclinic
formula weight	1052.89	1112.94	611.55	596.36	2456.14	3578.23	446.29
space group	$C2/c$	$P2_1/n$	$P\bar{1}$	$P2/c$	$P2_12_12$	$P2_1/n$	$P\bar{1}$
a/Å	21.116(12)	10.1476(19)	9.643(4)	12.1884(15)	18.6769(17)	13.7604(14)	9.808(3)
b/Å	19.219(11)	17.459(3)	11.553(5)	7.5019(9)	19.7262(18)	19.380(2)	9.898(3)
c/Å	16.261(10)	15.2450(19)	13.422(5)	28.691(4)	17.2957(15)	15.9509(17)	11.848(5)
α/°	90	90	83.300(14)	90	90	90	94.978(10)
β/°	127.888(18)	92.143(4)	87.442(15)	100.516(4)	90.00	113.614(3)	108.088(11)
γ/°	90	90	81.153(15)	90	90	90	115.629(7)
V/Å^3	5208(5)	2699.0(7)	1466.9(11)	2579.3(5)	6372.2(10)	3897.5(7)	952.4(5)
reflections collected	32 097	50 456	19 427	33 415	118 663	45 393	12 774
unique reflections	4983	9965	6246	5931	20 936	10 733	4195
observed reflections [$I > 2\sigma(I)$]	2615	5708	2476	2715	8348	9579	3430
R_1 [$I > 2\sigma(I)$]	0.0686	0.0575	0.0752	0.0790	0.0603	0.0450	0.0378
wR_2 [$I > 2\sigma(I)$]	0.1434	0.1363	0.1564	0.1726	0.1319	0.1131	0.1076
CCDC no.	984 410	984 408	984 407	984 411	984 406	984 412	984 409

FT-IR spectra were obtained on a Nicolet MAGNA-IR 750 spectrometer with a resolution up to 0.125 cm^{-1}. Thermal analyses were carried out with a TA Instruments SDT Q600 under nitrogenous atmosphere with a flow rate of 100 mL/min. Magnetic data were collected by MPMS (Evercool, 7 T) by Quantum Design, and C, H, and N microanalyses were carried out with a 2400 Series-II CHN analyzer, Perkin Elmer, USA, and CD spectra were collected using a JASCO J-815 CD spectrometer.

Synthesis of (1). Aqueous solution of $CoCl_2$, $6H_2O$ (0.0237 g, 0.1 mmol) was added dropwise to the mixed solution of H_2XBP (0.0148 g, 0.05 mmol) and terephthalic acid (0.0166 g, 0.1 mmol) dissolved in a 1:1 methanol DMF mixture. It was then heated to 80 °C in a sealed container for 72 h. After cooling, purple, block-shaped crystals were obtained which were filtered, washed with methanol, and dried in air (yield 45% based on H_2XBP).

IR (KBr, cm^{-1}): 3599.29 (sm), 3414.12 (br), 2924.18 (m), 2825.81 (sm), 1575.89 (m), 1386.86 (s), 1356.00 (s), 1186.26 (m), 1062.81 (m), 1012.66 (s), 831.99 (s).

Anal. Calculated for $C_{52}H_{54}Co_2N_8O_9$: C, 59.26 (59.54); H, 5.12 (4.91); N, 10.64 (10.50).

Synthesis of (2). Synthetic procedure of this compound was same as **1**. Isophthalic acid (0.0166 g, 0.1 mmol) was used as the corresponding ligand. Crystals obtained after cooling were block-shaped and purple in color. They were filtered and washed with methanol, and dried in air (yield 50% based on H_2XBP).

IR (KBr, cm^{-1}): 3275.24 (br), 2924.18 (sm), 1614.47 (s), 1388.79 (w), 1361.79 (s), 1286.56 (w), 1161.19 (sm), 1033.88, 752.26 (s), 723.33 (s).

Anal. Calculated for $C_{54}H_{58}Co_2N_8O_{11}$: C, 58.22 (58.65); H, 5.21 (5.35); N, 10.06 (10.11).

Synthesis of (3). This compound was synthesized the same way as **1** except diphenic acid (0.0242 g, 0.1 mmol) was used instead of TPA. After cooling purple, plate-shaped crystals were obtained which were filtered, washed with methanol, and dried in air (yield 49% based on H_2XBP).

IR (KBr, cm^{-1}): 3255.26 (br), 2862.51 (br), 1448 (s), 1239.21 (s), 1061.29 (s).

Anal. Calculated for $C_{32}H_{32}CoN_4O_5$: C, 62.80 (62.31) ; H, 5.23 (5.17) ; N, 9.15 (8.93).

Synthesis of (4). This compound was synthesized the same way as **1** except 4,4′-(hexafluoroisopropylidene) bis (benzoicacid) (0.0166 g, 0.1 mmol) was used as the corresponding ligand. Violet, plate-shaped crystals were obtained after cooling the container to room temperature in undisturbed way, which were filtered, washed with methanol, and dried in air (yield 52% based on H_2XBP).

IR (KBr, cm^{-1}): 3360.11 (s), 1610.61 (w), 1589.40 (m), 1410.01 (s), 1176.62 (s).

Anal. Calculated for $C_{26}H_{19}CoF_6N_2O_4$: C, 52.3 (52.14); H, 3.18 (3.40); N, 4.69 (4.95).

Synthesis of (5). Same procedure as **1** was repeated to prepare this compound expect using 4,4′-oxybis(benzoicacid) (0.0258 g, 0.1 mmol) in place of TPA. Purple-colored, plate-shaped crystals were obtained, filtered, washed with methanol, and dried in air (yield 55% based on H_2XBP).

IR (KBr, cm^{-1}): 3408.33 (br), 2926.11 (br), 1597.11 (s), 1384 (s), 1238.34 (s), 1161.19 (s), 1012.66 (s), 777.34 (sm).

Anal. Calculated for $C_{128}H_{122}Co_4N_{16}O_{21}$: C, 62.53 (62.10) ; H, 4.96 (4.82) ; N, 9.12 (9.10).

Synthesis of (6). Exactly same procedure as **1** was performed to prepare this compound except using trimesic acid (0.0210 g, 0.1 mmol) as the corresponding acid, and the reaction temperature was increased to 120 °C. Crystals obtained after cooling were pink in color and block in shape. They were filtered, washed with methanol, and dried in air (yield 45% based on H_2XBP).

IR (KBr, cm^{-1}): 3424.3 (br), 2852.10 (br), 1726 (s), 1680.16 (s), 1614.77 (s), 1554.68 (s), 1540.11 (s), 1423.11 (s), 1202.55 (s).

Anal. Calculated for $C_{148}H_{144}Co_8N_{16}O_{60}$: C, 49.63(50.88); H, 4.02 (3.94); N, 6.25 (5.85).

Synthesis of (7). Purple, block-shaped crystals of **7** were obtained maintaining the same composition of the reacting substances and the same solvent system as for compound **6**. Only the temperature was decreased from 120 to 80 °C. The crystals were filtered, washed with methanol, and dried in air (yield 46% based on H_2XBP).

IR (KBr, cm^{-1}): 3244.38 (br), 2931.90 (br), 1691.63 (s), 1614.47 (s), 1554.68 (s), 1440.87 (s), 1373.36 (s), 1292.35 (s), 1035.81 (s), 721.40 (s).

Anal. Calculated for $C_{19}H_{19}CoN_2O_7$: C, 51.08 (50.60); H, 4.25 (4.15); N, 6.27 (6.21).

X-ray Crystallography. X-ray diffraction intensities were collected at 120 K on Bruker APEX-2 CCD diffractometer using Mo−K_∞ radiation and processed using SAINT. The structures were solved by direct methods in SHELXS and refined by full matrix least-squares on F^2 in SHELXL.[17] All non-hydrogen atoms were refined with anisotropic thermal parameters. The hydrogen atoms are located on a difference Fourier map and refined isotropically. In other cases, the hydrogen atoms are geometrically fixed. For compound **2**, the bis pyrazole ligand molecule shows a considerable amount of positional disorder. Twelve carbon atoms (C7 to C18) of the central benzene ring and one of the pyrazole ring show disorder with 50% site occupancy for both the components. Crystallographic data are summarized in Table 1, and CIF files for the structures reported in this paper have been deposited with the Cambridge Crystallographic Data Centre (CCDC). Deposition numbers are given in Table 1. Copies of the data can be obtained, free of charges, on application to

the CCDC, 12 Union Road, Cambridge, CB2 1EZ, UK (Fax 44 (1223)336 033; e-mail: deposit@ccdc.cam.ac.uk).

RESULT AND DISCUSSION

Complexes **1**−**7** were synthesized by a hydrothermal method under similar conditions using $CoCl_2$, $6H_2O$, H_2XBP, and corresponding acids in 2:1:2 molar ratios. All the complexes were characterized by elemental analysis, IR spectroscopy, and X-ray single crystal diffraction analysis.

One of the major advantages of using 1-H-pyrazole based ligands is their singular ability to force carboxylate groups to one particular coordination mode. The metal coordinated pyrazole moiety, with the presence of an in-built hydrogen bonding site, almost invariably forms a H-bond with the second oxygen atom of the monodentate carboxylate group (Scheme 1), which in turn restricts the metal-carboxylate cluster formation. We have verified this occurrence with a large number of crystal structures of coordination polymers using mixed ligand systems of carboxylic acid and pyrazole based coordination ligands. These pyrazole-carboxylate hydrogen bonded motifs and restriction of metal-carboxylate cluster formation are the basis of this study, and except for a partial deviation in **7**, we did not find any exception to this trend.

Structural Description. Single crystal X-ray diffraction analysis shows that compound **1** crystallizes in the centrosymmetric *C*2/*c* space group and is composed of a 4-fold interpenetrated diamondoid network. Its asymmetric unit consists of a cobalt atom, one terephthalate ion, and two symmetry independent half molecules of H_2XBP, along with a noncoordinated water molecule. The cobalt atom adopts a tetrahedral geometry and coordinated to two nitrogen atoms from two H_2XBP molecules and two oxygen atoms of the carboxylate groups of the TPA anion. As expected, the carboxylate groups of the TPA adopt a "locked" monodentate mode with the second uncoordinated oxygen atom forming a characteristic N−H/O bond with the H_2XBP molecule. From a topological viewpoint, the resultant three-dimensional framework can be assigned as a diamondoid network by considering the metal centers as nodes (Figure 1) with a reasonably large dimension of ca. 38.44 Å × 32.47 Å × 25.69 Å. A diamondoid network with such a large cavity usually tends to undergo interpenetration, and the crystal structure of **1** was not an exception. A closer inspection of the structure reveals a 4-fold interpenetration of the network. These interpenetrating diamondoid networks are further connected by $O-H\cdots O_{water}$ and $O_{water}-H\cdots O$ bonds between carboxylate groups and the guest water molecule, while further assistance came from several $\pi-\pi$ interactions among aromatic rings of H_2XBP and TPA molecules.

The reaction between H_2XBP and cobalt-nitrate in the presence of isophthalic acid results in single crystals of $\{[Co(H_2XBP)(IPA)]\cdot(H_2O)(CH_3OH)\}$, compound **2**. The asymmetric unit of **2** contains a cobalt(II) center, an IPA anion, a disordered H_2XBP ligand, one each of noncoordinated methanol and water molecule. The Co(II) ion is coordinated to two oxygen atoms from two IPA anions and two nitrogen atoms from two H_2XBP ligands to furnish a tetrahedral coordination. Compound **2** has an unusual (4,4) grid network, considering the metal center as a node. Interestingly, unlike most of the 2D (4,4) grid networks, it is not planar but undulated, resulting from an interesting self-assembly of ligand molecules while coordinating to the metal center (Figure 2). The grid network can also be described in terms of the self-

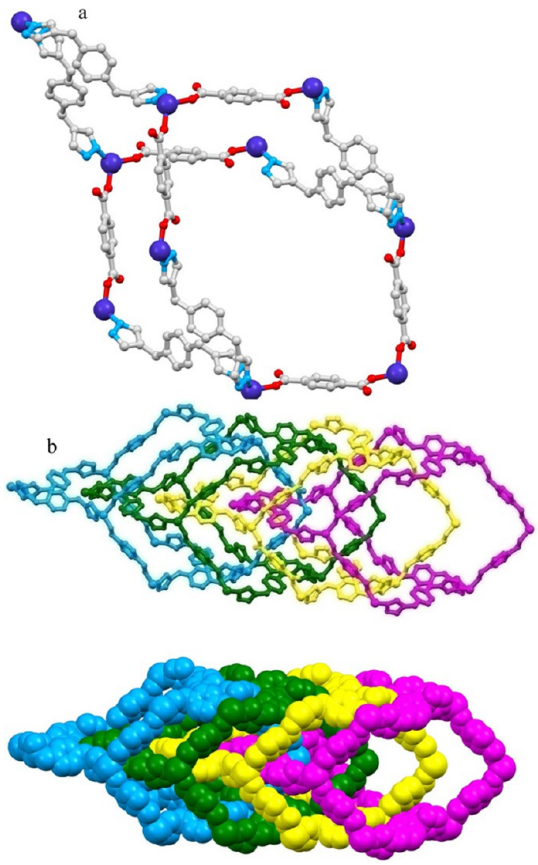

Figure 1. Crystal structure of **1** showing (a) the basic diamondoid network and (b) 4-fold interpenetrated diamondoid network in a ball−stick and space-filled model.

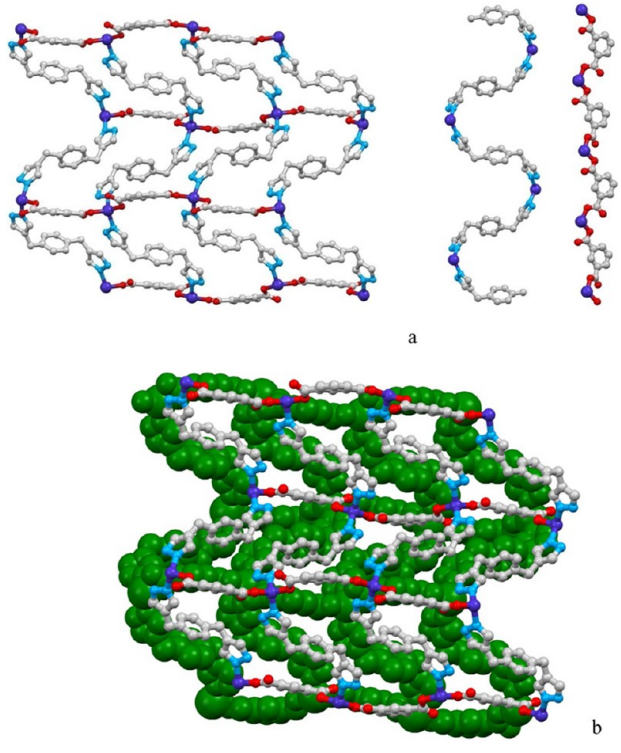

Figure 2. Crystal packing of **2** showing (a) an undulated (4,4) type grid network along with two intersecting 1D networks and (b) offset stacking of these grid networks.

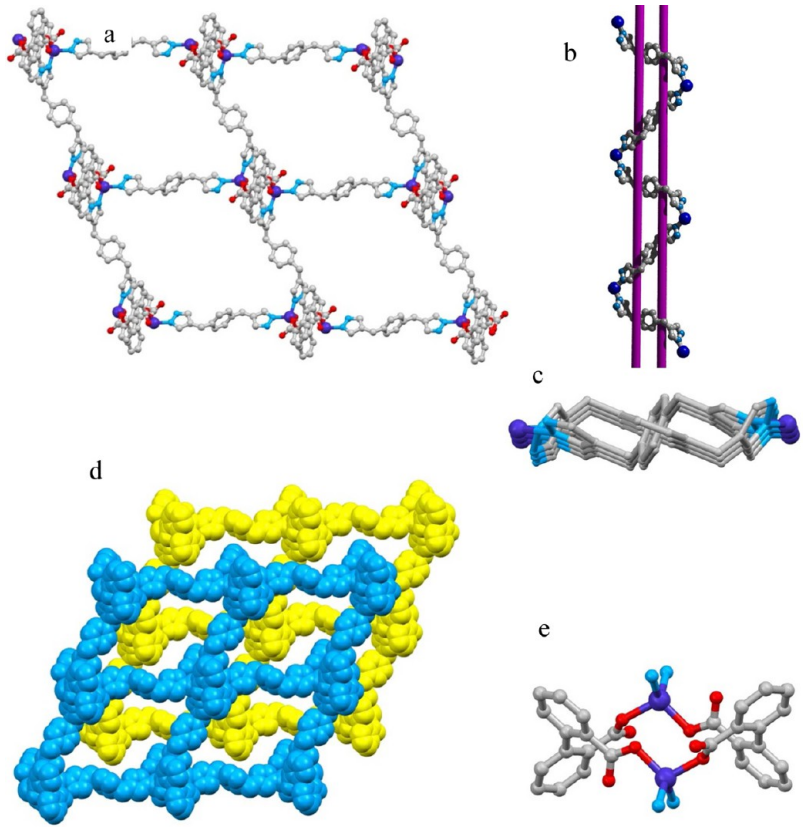

Figure 3. (a) (4,4) Type 2D grid network of compound **3**, (b) mesohelical chain, (c) top view of the mesohelical chain, (d) offset stacking of the grids, (e) binding fashion of DPA molecule in compound **3**.

assembly to two intersecting 1D networks, parallel strands of vertically expanded helices of metal coordinated H_2XBP molecules and a linear chain of IPA molecules expanding in the horizontal direction. Furthermore, these wavelike sheets undergo offset stacking, sustained by several N−H···O and O−H···O_{MeOH} bonds and $\pi-\pi$ stacking. Another interesting feature of the structure is the relatively larger size of the grid with a dimension of 19.39 Å × 9.38 Å, which could be attributed to the longer length of the H_2XBP molecule.

Replacement of isothalic acid with diphenic acid leads to another interesting (4,4) type grid network for compound **3** that crystallizes in triclinic $P\bar{1}$ space groups, and the asymmetric unit contains one cobalt atom, one DPA anion, two asymmetry independent half molecules of H_2XBP, and one lattice water molecule. The Co(II) ion adopts a tetrahedral geometry and coordinated to two oxygen atoms from two DPA anions and two nitrogen atoms from two H_2XBP ligands. Interestingly, two DPA molecules with a V-shaped arrangement of the carboxylate groups coordinate to metal centers in a monodentate fashion and lead to the formation of a centrosymmetric dinuclear Co(II) metallocyclic unit with a Co/Co distance of 4.31 Å (Figure 3). The H_2XBP molecules, on the other hand, bridge these dinuclear units to generate a 2D grid network, which can also be denoted as a (4,4) type network considering the dinuclear metallocyclic units as nodes. Again, the larger size of H_2XBP manifests in an unusually large grid network with a dimension of 23.32 Å × 19.40 Å (considering diagonal Co···Co distances). Effective pore size, however, was reduced considerably because of offset stacking of the grids, which is further sustained by extensive intergrid $\pi-\pi$ interactions.

Another fascinating feature of compound **3** is the presence of a not-so-common meso-helical motif, a special type of helical chain where right- and left-handed helices are formed in equal amounts within a single helical chain. As illustrated in Figure 3, metal-coordinated propagation of H_2XBP molecules represents a meso-helical chain with the coexistence of both left- and right-handed helical motifs.

Inspired by the above structure, compound **4** was synthesized using H_2FBA as an auxiliary ligand. H_2FBA being another bent ligand has a natural tendency to form helical network and has often been used as a strategic tool to introduce helicity in the resultant polymeric network. Indeed, compound **4** forms an interesting three-dimensional helical network. Compound **4** crystallizes in monoclinic $P2/c$ space group, and the asymmetric unit contains one-half of two cobalt atoms, one FBA molecule, and one-half of a H_2XBP molecule. Interestingly, carboxylate groups of the FBA molecules adopt two distinctly different kinds of coordination modes: a bidentate bridging one and another tridentate chelating/bridging mode. Such coordination modes result in two completely different coordination environments around the two symmetry independent octahedral cobalt atoms. While one of the cobalt atoms is coordinated to six oxygen atoms of four carboxylate groups, the other one is coordinated to two nitrogen atoms of two H_2XBP molecules along with four oxygen atoms of four carboxylate groups. Subsequently, the cobalt atoms are unidirectionally bridged by an alternative pair of bidentate and tridentate carboxylate groups, which led to a single-strand chain of cobalt atoms. Such a single-strand chain of cobalt atoms are immensely important from a magnetic exchange interaction point of view, and as

dx.doi.org/10.1021/cg500174g | *Cryst. Growth Des.* 2014, 14, 2853−2865

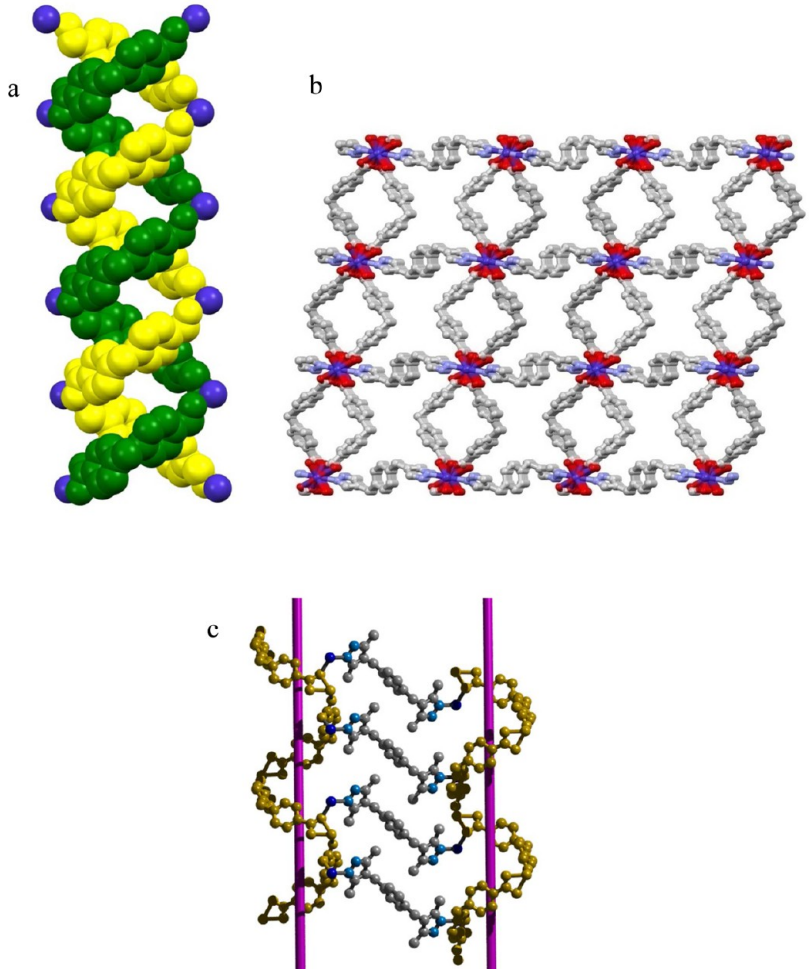

Figure 4. (a) Helical motif present in compound **4**, (b) packing pattern of compound **4**, (c) different handed helical chains connected by H_2XBP molecule.

discussed in the later section, compound **4** indeed shows some interesting magnetic behavior.

Topologically, a complex three-dimensional framework was formed when H_2XBP and FBA molecules connect these single-strand chains and expand in horizontal and vertical directions, respectively. As illustrated in Figure 4, the resultant network can also be described in two parts: a parallel arrangement of one-dimensional nanochannels made of FBA molecules, while the H_2XBP molecules act as linker and connect the nanochannels horizontally.

However, the most fascinating aspect of the structure is the nature of helicity introduced by the V-shaped H_2FBA molecules. A closer inspection of the nanochannels would reveal that they are actually constructed by interweaving double helical chains. Interestingly, the individual double helical networks resulted with a combination of two helical chains of one particular handedness; i.e., either we have a left-handed or a right handed double helical network. On the other hand, the two juxtaposed double helical chains, constructed by the H_2XBP molecule, at the two ends, are of different handedness; i.e., if one of the double helical chain is left handed the other one is a right handed. It is noteworthy here that such occurrence of two interconnected double-helical chains with different handedness is not so common even though a plethora of helical chain is known in the literature.

Introduction of H_2OBA, another well-known V-shaped ligand, however results in an interesting 5-fold interpenetrated diamondoid network for compound **5** (Figure 5). Compound **5** crystallizes in orthorhombic $P2_12_12$ space group with two cobalt atoms, two H_2XBP molecules, one full and two symmetry independent half molecules of OBA, and one noncoordinating water molecule in the asymmetry unit. The cobalt atoms adopt tetrahedral geometry and are coordinated to two oxygen atoms of two OBA anions and two nitrogen atoms from two H_2XBP molecules. It has been observed that metal centers with coordination number four have a high propensity to form diamondoid networks, and compound **5** was no exception. Structural analysis of the three-dimensional framework reveals a diamondoid network by considering the metal center as nodes with a dimension of 46.70 Å × 36.43 Å × 26.23 Å. As expected, the large cavity formed inside resultant diamondoid network leads to 5-fold interpenetration, while the larger dimension and higher degree of interpenetration for compound **5**, compared to those of compound **1**, can be attributed to the longer length of the OBA molecule with respect to terephthalate anion.

With H_2TMA as an auxiliary ligand, two distinctly different colored compounds, pink-colored **6** and purple-colored **7**, were obtained when reactions were carried out at 120 and 80 °C, respectively. A comparative structural analysis reveals two important points: different coordination modes of H_2TMA

dx.doi.org/10.1021/cg500174g | *Cryst. Growth Des.* 2014, 14, 2853−2865

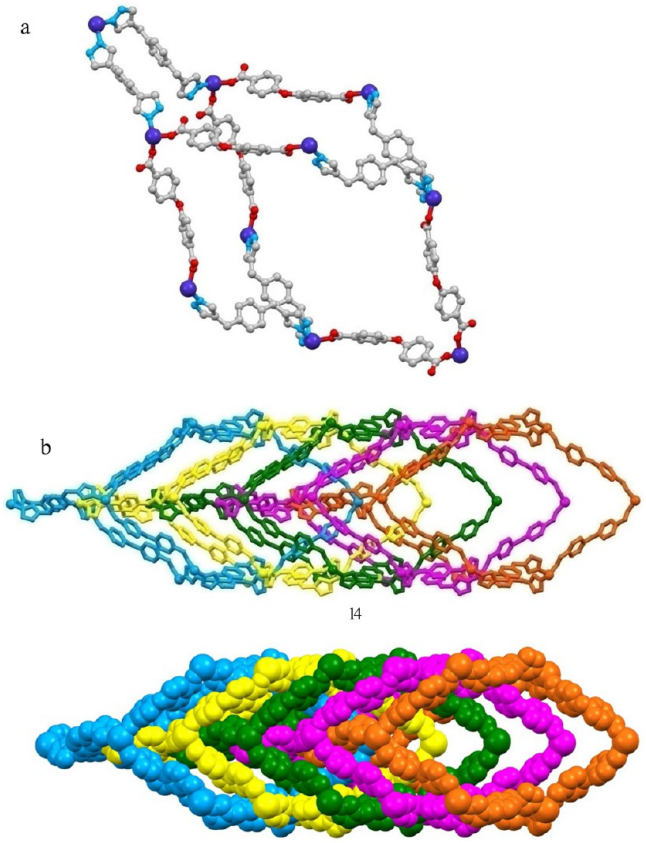

Figure 5. View of **5** showing (a) the basic diamondoid network and (b) 5-fold interpenetrated diamondoid network in a ball−stick and space-filled model.

molecule and two distinctly different conformations of H_2XBP. Compared to three metal coordinated carboxylates groups of **6**, only two carboxylate groups coordinate to metal centers in **7**, while the third one remains protonated and takes part in hydrogen bond formation. Another distinguishing feature between compounds **6** and **7** is the different conformations adopted by the H_2XBP molecules, a *cis* and a *trans* (Figure 6),

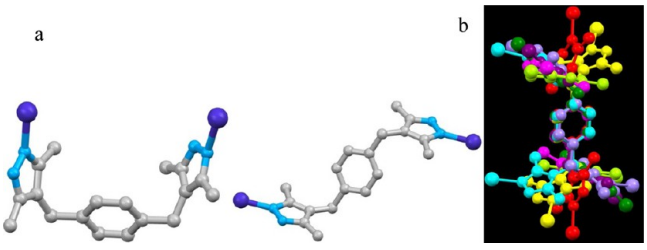

Figure 6. (a) *Cis* and *trans* conformation of H_2XBP molecule (b) superimposed picture of the conformations of H_2XBP in compound **1**−**7**.

respectively. This also raises another interesting issue of the influence of conformational freedom of a ligand molecule on the resulting network, which deserves to be discussed in a little more detail.[11,12] The H_2XBP molecule has two methylene groups between the pyrazole moieties and central benzene ring which allows H_2XBP to have flexible conformations and better adaptability. Apparently, depending on the requirements the H_2XBP molecule can adopt different conformations via bending, stretching, or twisting about the $C(sp^3)-C(sp^2)$ bond (Figure 6). A superimposed picture of H_2XBP molecules corresponding to **1**−**7** can further simplify this point. Each of these molecules adopts different conformations, required for a particular network formation, and further speaks for the advantages of using flexible ligands. Of particular interest is the distance between the metal atoms or coordinating sites of the ligand which can play a decisive role in tuning the dimension of a network, especially when metals centers are considered as the vertices of the network.

Compound **6** crystallizes in monoclinic $P2_1/n$ space group with two cobalt atoms, one H_2XBP molecule with a *cis* conformation, two TMA molecules, two coordinated water molecule, and one free methanol molecule in the asymmetric unit. A detail structural analysis shows a highly unusual two-dimensional topology. The TMA anion, with a C_3 symmetry, coordinates to three metals centers which can be considered as the vertices of an equilateral triangle. Subsequently, the network can be simplified as an infinite expansion of these conjoined triangles. The H_2XBP molecule with a hairpin-like conformation, on the other hand, clips one of the sides of the triangle. This results in an unusual two-dimensional network with an infinite triangular lattice of coplanar cobalt atoms with dangling H_2XBP molecules. It is interesting note here that the hanging H_2XBP molecules were occupied only on one side of the plane. Furthermore, as depicted in Figure 7, these dangling H_2XBP molecules undergo interesting interdigitations to generate the three-dimensional supramolecular structure supported by several hydrogen bonds and $\pi-\pi$ interactions.

A slight variation in reaction conditions with H_3TMA as auxiliary ligand results in purple-colored crystals of compound **7**. However, both H_2XBP and acid show some subtle differences than those observed in compound **6**. While H_2XBP molecule adopts a more familiar *trans* conformation, only two carboxylate groups of the trimesic acid coordinate to the metal center while the unligating third one remains protonated. Furthermore, the two ligating carboxylate groups adopt different coordination modes; one of them was monodentate while the second one remains monodentate but bonded to two metals ions with an unusual *syn-anti* coordination mode. Such *syn*−*anti* coordination mode of the carboxylate group results in a centrosymmetric binuclear cluster formation, which is further interconnected by the second monodented carboxylate groups. This effectively results in parallel strands of one-dimensional double decker chains of acid molecules supported by strong $\pi-\pi$ staking. On the other hand, coordination of two H_2XBP molecules at the two ends of the centrosymmetric cluster results in a planar two-dimensional coordination network while one methanol molecule occupies an apical position of the trigonal bipyramidal metal center.

Furthermore, the crystal structure of compound **7** exhibits an interesting supramolecular self-assembly if we take hydrogen bonding of the third carboxylic groups into consideration. As illustrated in Figure 8, the carboxylic acid groups of two adjacent 2D gird networks come very close to each other and from a characteristic hydrogen bonded acid dimer and results in a hexagonal net with a chicken wire pattern.[18] It is noteworthy here that although chicken wire type self-assembly of trimesic acid is well-known most of them are driven by H-bonding. Compound **7**, therefore, represents a unique self-assembly of trimesic acid where a chicken wire pattern was achieved by combined exploitation of both hydrogen bonds as well as metal coordination.

dx.doi.org/10.1021/cg500174g | *Cryst. Growth Des.* 2014, 14, 2853−2865

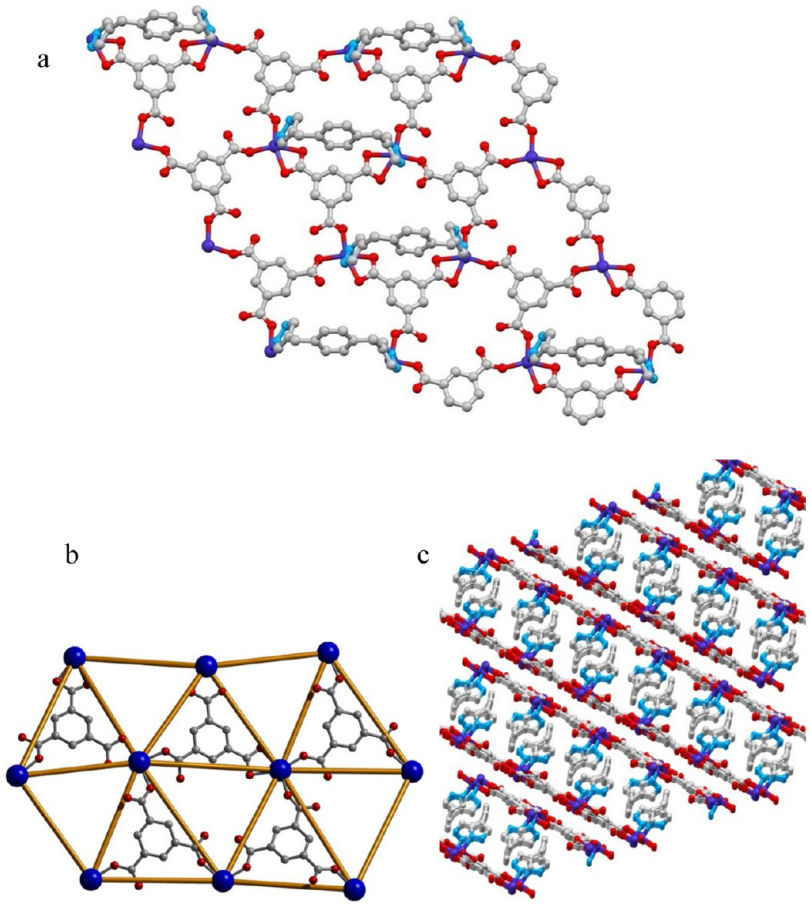

Figure 7. Crystal structure of **6** showing (a) 2D grid network, (b) alternative positions of TMA in conjoined triangles (the H_2XBP molecules are omitted for clarity), (c) three-dimensional packing with the interdigitations of H_2XBP molecules.

Magnetic Property. The temperature and field dependent molar magnetic susceptibility of compound **4** was measured from 2 to 300 K by using crushed microcrystalline solid in a magnetic field of 200 and 1000 Oe. The $\chi_M T$ value at 300 K per Co unit (2.29 $cm^3\ mol^{-1}\ K$) is higher than the expected spin-only value for $S = 3/2$ (1.875 $cm^3\ mol^{-1}\ K$, $g = 2.0$), attributed to the orbital contribution arising from Co^{II} center. Upon cooling from room temperature, the $\chi_M T$ value decreases smoothly down to 1.43 $cm^3\ mol^{-1}\ K$ at 10 K and then increases slowly to reach a value 1.49 $cm^3\ mol^{-1}\ K$ at 2 K.

The magnetic behavior in the temperature range of 20 K–300 K follows the Curie–Weiss Law with a negative Weiss constant (θ) = −19.2 K and a Curie constant of 2.38 $cm^3\ mol^{-1}$ K, which corresponds to a spin $S = 3/2$ with a g value higher than 2.

Zero field cooled (ZFC) and field cooled (FC) magnetic susceptibility measurements were performed in the temperature range 2.0–300.0 K. The two curves are almost super positioned until ∼50 K with a bifurcation below about 50 K. The field-dependent isothermal magnetization $M(H)$ was performed at 3, 100, and 200 K. As shown in Figure 9 an abrupt linear increase of magnetization at 100 and 200 K to a value of about 1.5 Nβ (at 200 K) is observed at 5 T. However, the $M(H)$ curve is different at 3 K compared to the curves at 100 and 200 K and it is somewhat S shaped.

The polymeric nature of the compound **7** can be easily simplified to a Co^{II} dimer skeleton as schematized as shown in Figure 10a, where J represents intradimer magnetic exchange interaction. The temperature dependent magnetic susceptibility measurement of powder sample of the complex in the range of 2–300 K is shown in Figure 10b, in the form of χ_m vs T and $\chi_m T$ vs T plots, χ_m being the corrected molar magnetic susceptibility per dimer unit. The $\chi_m T$ value of complex does not vary significantly up to 80 K from room temperature before a sudden drop at lower temperature, indicating antiferromagnetic behavior of the compound. The room temperature value of per Co^{II} dimer (6.45 $cm^3\ K\ mol^{-1}$) is larger than that calculated for the spin-only case (3.75 $cm^3\ K\ mol^{-1}$), indicating strong orbital contribution as frequently observed in other Co^{II} complexes. It is quite difficult to estimate the accurate exchange interaction within Co^{II} metal ions where significant spin–orbit coupling involved. Here, we considered an admittedly simple dimer model and assumed only spin contribution predominates with the isotropic g parameter. The temperature dependence of the magnetic susceptibility for complex is assumed mainly due to intradimer exchange interaction (J), where two Co^{II} ions are bridged by two carboxylate moieties, and interdimer exchange interaction (J'). So the intradimersusceptibility (χ_{dimer}) as given in eq 1 can be approximated to eq 2 by considering interdimer interaction as well as temperature independent paramagnetism (α)[19]

$$\chi_{dimer} = \frac{2N^2g^2}{kT}\left[\frac{e^{-10x} + 5e^{-6x} + 14}{e^{-12x} + 3e^{-10x} + 5e^{-6x} + 7}\right] \quad (1)$$

dx.doi.org/10.1021/cg500174g | Cryst. Growth Des. 2014, 14, 2853–2865

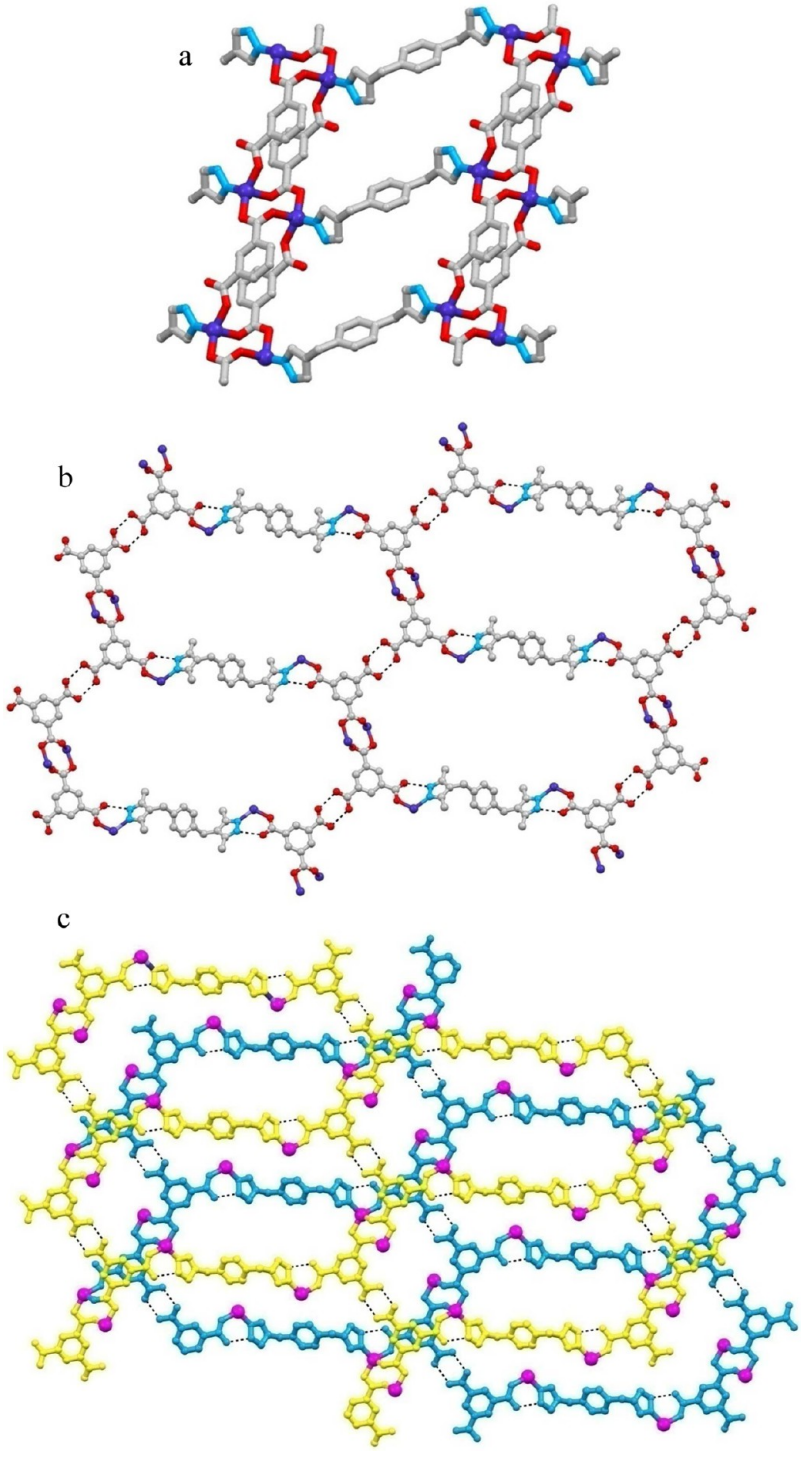

Figure 8. (a) Basic network of compound **7** showing binuclear clusters (one carboxylate group is omitted for clarity), (b) view of H-bonded hexameric chicken wire pattern, and (c) offset stacking of the chicken wire type networks.

$$\chi = \frac{\chi_{\text{dimer}}}{1 - \left[\frac{2zJ'}{N\beta^2 g^2}\right]_{\text{dimer}}} + (\text{TIP}) \qquad (2)$$

where z is the number of nearest neighbors of the dimers (four in this case) and $x = J/kT$. The N, β, g, k, and T terms have their usual meanings. The best possible value of g, J, J', and α were obtained by the nonlinear least-squares fittings of the experimental $\chi_m T$ vs T data by eq 2 and minimizing the residual $R = [\Sigma(\chi_{obs}T - \chi_{calc}T)^2/\Sigma(\chi_{obs}T)^2]$. The best fit parameters are $J = -2.35\ \text{cm}^{-1}$, $J' = -0.00687\ \text{cm}^{-1}$, $g = 2.45$, $\alpha = 0.005$, and $R = 3.6 \times 10^{-5}$. The larger value of the g parameter may be due to significant orbital effect; otherwise it seems that the spin-only model gives quite a good fit. The simulated $\chi_m T$ vs T for different g values are given in Supporting information (Figure S2).

CD Spectra of Compound 4. Interaction between circularly plane polarized light with chiral matter and consequential difference in the absorption of left and right circularly polarized light at the vicinity of the absorption band

dx.doi.org/10.1021/cg500174g | *Cryst. Growth Des.* 2014, 14, 2853−2865

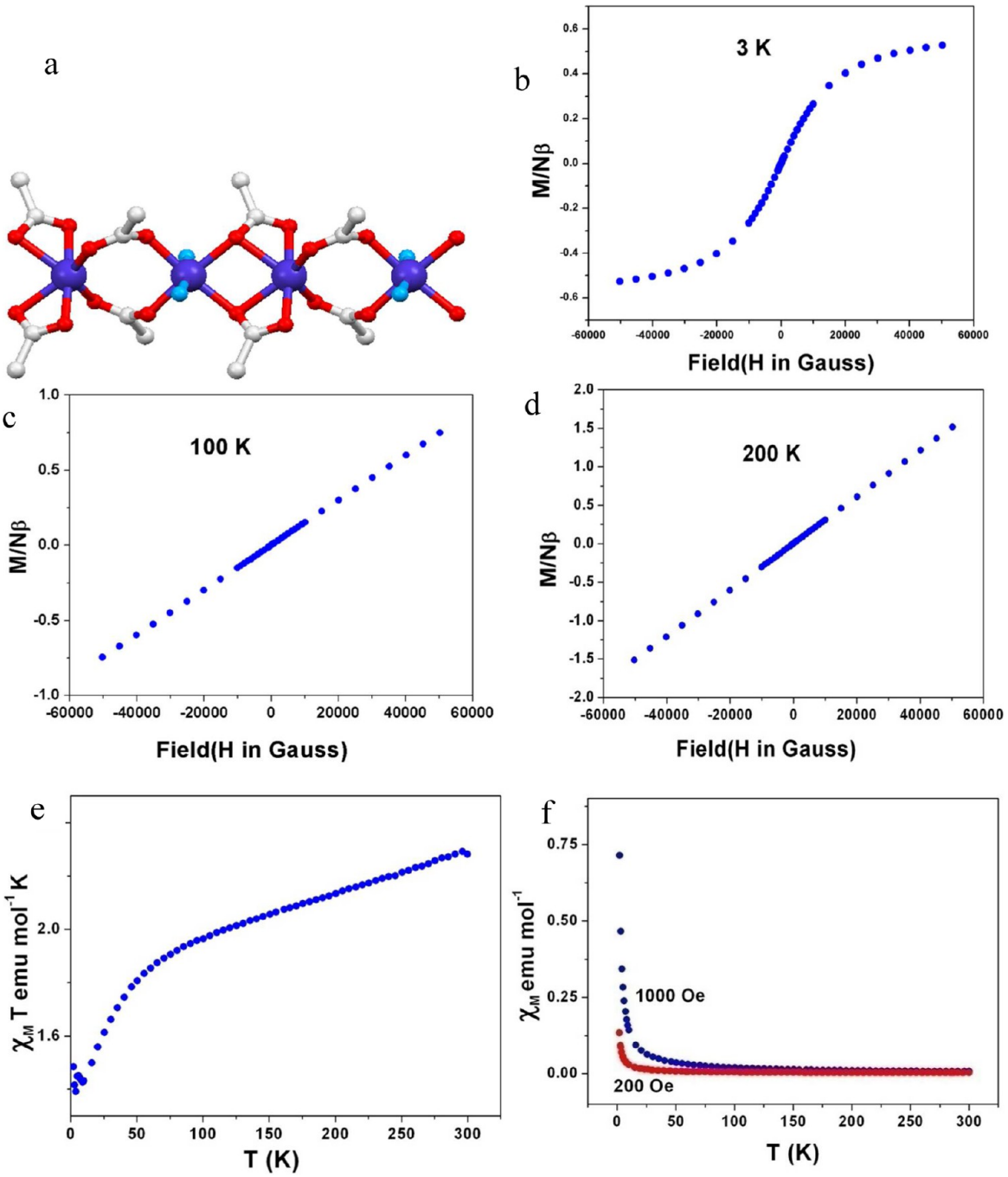

Figure 9. (a) Carboxylate bridged 1D metal cluster of compound **4**. Magnetization $M(H)$ of compound **4** performed at (b) 3 K, (c) 100 K, (d) 200 K. (e and f) Temperature dependence of χ_m and $\chi_m T$ of the compound.

of the optically active substance paved the way for so-called Cotton effect.[20] The presence of helical motif is often known to induce chirality in a MOF even though the ligand molecules used for the synthesis are achiral.[18] After discovering the presence of intriguing helical motif in structure of compound **4,** we were interested to study its chirality. Accordingly we recorded solid state CD spectra of the compound in a diffuse reluctance technique over KBr matrix at room temperature. The compound exhibits the Cotton effect showing two broad signals at 580 and 358 nm as shown in Figure 11. Origin of chirality is attributed here by the presence of helical chains. It is well-known that helicity can play a crucial role to induce chirality in a molecule.[18] Interestingly, two same handed intertwined helical motifs are present in this compound which actually plays an additive role to confirm spontaneous resolution at the time of crystallization. Again repetition of same CD spectra from different batches of compounds supports the formation of enantiomerically pure compound.

Thermogravimetric Analysis. Considering the fact that azole based MOFs are well-known for their high thermal stability, we investigated the thermal analysis of all the compounds of this work. All the samples were heated in a platinum crucible at a rate of 10 °C m^{-1} under nitrogenous atmosphere within the temperature range of 25−800 °C (Figure 12). Compound **1** showed about 10% weight loss at ∼310 °C. For compound **2** at about 90 °C, 10% weight loss was

dx.doi.org/10.1021/cg500174g | *Cryst. Growth Des.* 2014, 14, 2853−2865

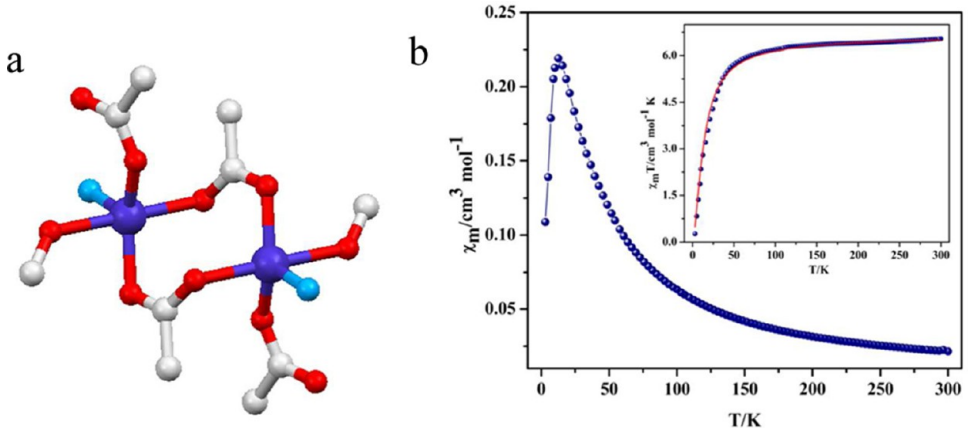

Figure 10. (a) Carboxylate bridged Co(II) dimer in compound **7**, (b) the plot showing temperature dependence of χ_m and $\chi_m T$ (inset) of the compound. The red solid line (inset) represents best fit of the $\chi_m T$ curve.

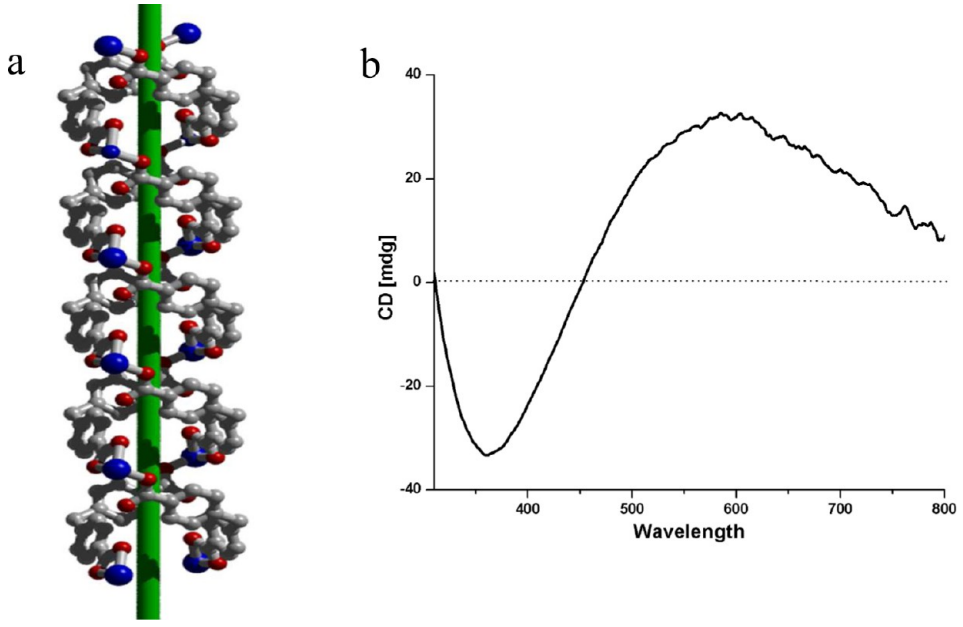

Figure 11. (a) Two same handed helical chains present in compound **4**, (b) solid state CD spectra of compound **4**.

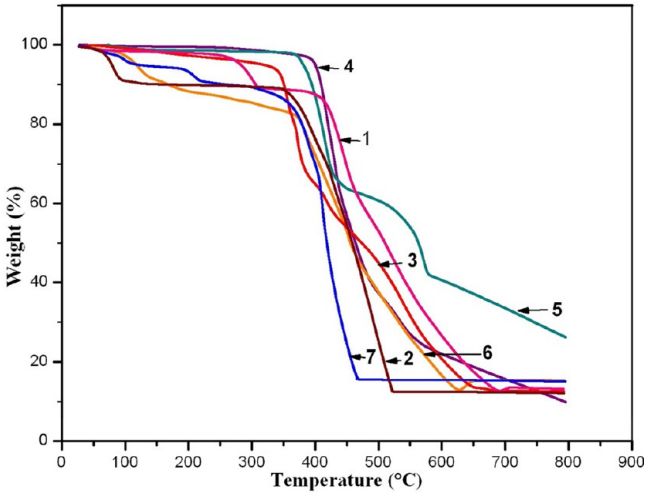

Figure 12. Thermogravimetric analysis of compounds **1**−**7**.

detected, and the compound started to decompose at ∼350 °C. Compound **3** was stable up to ∼345 °C. Compound **4** was highly stable and started to decompose at about 400 °C. For compound **5** two step weight loss was observed. An initial 34% weight loss was observed at ∼435 °C followed by another 58% weight loss at ∼577 °C. Compound **6** showed 4.5% decomposition at ∼108 °C and 8.49% decomposition at ∼213 °C and finally started to decompose at ∼360 °C. For compound **7** about 7% weight loss was found at ∼128 °C, and at ∼374 °C the compound started to degrade.

CONCLUSION

The impetus for the work presented herein was to validate the usefulness of 1-H pyrazole based bridging ligands in multifunctional MOF synthesis. Accordingly, we have successfully synthesized a series of Co(II) coordination polymers constructed from a flexible neutral pyrazole based ligand and benzene polycarboxylic acids. One of the most fascinating outcomes of this work is construction of diverse structural networks, from a two-dimensional bilayer network to grid, nanoporous channels, an unusual supramolecular chicken-wire

dx.doi.org/10.1021/cg500174g | *Cryst. Growth Des.* 2014, 14, 2853−2865

type network to three-dimensional diamondoid network. We have also shown that the conformational freedom of the ligand plays a crucial role in the determining both the dimensionality and topology of the final structure. One of the promising features of these MOFs is their unusual yet consistent larger dimensions, which enhances the possibility of increased porosity and well-defined cavity within the network. The thermogravimetric analyses of the MOFs show a reasonably high thermal stability. We have also successfully demonstrated our strategy of using a V-shaped ligand for generating helical MOF, with the enhanced possibility of inducing chirality in the framework. Furthermore, solid state CD spectra and magnetic properties highlight the potential applications of these compounds as chiral and magnetic materials.

■ ASSOCIATED CONTENT

Ⓢ Supporting Information

Mass spectra of H_2XBP ligand, selected bond lengths and bond angles for compounds **1**−**7**, simulated and experimental powder patterns of compounds **1**−**7**, simulated plot of $\chi_m T$ vs T for different values of g, table of thermogravimetric analysis, and crystallographic information in CIF format. This material is available free of charge via the Internet at http://pubs.acs.org.

■ AUTHOR INFORMATION

Corresponding Author

*E-mail: icrm@iacs.res.in.

Notes

The authors declare no competing financial interest.

■ ACKNOWLEDGMENTS

R.M. gratefully acknowledges Science and Engineering Research Board (SERB) (Project No. SR/S1/IC-65/2012) India, for financial assistance. Sudeshna Bhattacharya, S.S.G., Sukhen Bala, and A.G. are thankful to CSIR, India, for research fellowships.

■ REFERENCES

(1) (a) Li, J.-R.; Kuppler, R. J.; Zhou, H.-C. *Chem. Soc. Rev.* **2009**, *38*, 1477−1504. (b) Sumida, K.; Rogow, D. L.; Mason, J. A.; McDonald, T. M.; Bloch, E. D.; Herm, Z. R.; Bae, T.-H.; Long, J. R. *Chem. Rev.* **2012**, *112*, 724−781. (c) Serra-Crespo, P.; van der Veen, M. A.; Gobechiya, E.; Houthoofd, K.; Filinchuk, Y.; Kirschhock, C. E. A.; Martens, J. A.; Sels, B. F.; De Vos, D. E.; Kapteijn, F.; Gascon, J. *J. Am. Chem. Soc.* **2012**, *134*, 8314−8317. (d) Collins, D. J.; Zhou, H.-C. *J. Mater. Chem.* **2007**, *17*, 3154−3160. (e) Liu, J.; Thallapally, P. K.; McGrail, B. P.; Brown, D. R.; Liu, J. *Chem. Soc. Rev.* **2012**, *41*, 2308−2322. (f) Horcajada, P.; Chalati, T.; Serre, C.; Gillet, B.; Sebrie, C.; Baati, T.; Eubank, J. F.; Heurtaux, D.; Clayette, P.; Kreuz, C.; Chang, J.-S.; Hwang, Y. K.; Marsaud, V.; Bories, P.-N.; Cynober, L.; Gil, S.; Férey, G.; Couvreur, P.; Gref, R. *Nat. Mater.* **2010**, *9*, 172−178. (g) Kaye, S. S.; Dailly, A.; Yaghi, O. M.; Long, J. R. *J. Am. Chem. Soc.* **2007**, *129*, 14176−14177. (h) Eddaudi, M.; Moler, D. B.; Li, H.; Chen, B.; Reineke, T. M.; Keeffe, M. O'; Yaghi, O. M. *Acc. Chem. Res.* **2001**, *34*, 319−330. (i) Nickerl, G.; Henschel, A.; Grünker, R.; Gedrich, K.; Kaskel, S. *Chem. Ingenieur Technol.* **2011**, *83*, 90−103. (j) Kurmoo, M. *Chem. Soc. Rev.* **2009**, *38*, 1353−1379.

(2) (a) Ghosh, S. K.; Azhakar, R.; Kitagawa, S. *Chem.—Asian J.* **2009**, *4*, 870−875. (b) Janiak, C.; Vieth, J. K. *New J. Chem.* **2010**, *34*, 2366−2388. (c) Férey, G. *Dalton Trans.* **2009**, 4400−4415. (d) Lin, C.-K.; Zhao, D.; Gao, W.-Y.; Yang, Z.; Ye, J.; Xu, T.; Ge, Q.; Ma, S.; Liu, D.-J. *Inorg. Chem.* **2012**, *51*, 9039−9044. (e) Chen, X.-D.; Wan, C.-Q.; Sung, H. H. -Y.; Williams, I. D.; Mak, T. C. W. *Chem.—Eur. J.* **2009**, *15*, 6518−6528.

(3) (a) Gurunatha, K. L.; Uemura, K.; Maji, T. K. *Inorg. Chem.* **2008**, *47*, 6578−6580. (b) Wang, S.; Li, L.; Zhang, J.; Yuan, X.; Su, C.-Y. *J. Mater. Chem.* **2011**, *21*, 7098−7104.

(4) (a) Steel, P. J. *Acc. Chem. Res.* **2005**, *38*, 243−250. (b) Burnett, B. J.; Barron, P. M.; Choe, W. *CrystEngComm* **2012**, *14*, 3839−3846. (c) Liu, L.; Wang, X.; Zhang, Q.; Li, Q.; Zhao, Y. *CrystEngComm* **2013**, *15*, 841−844. (d) Barman, S.; Furukawa, H.; Blacque, O.; Venkatesan, K.; Yaghi, O. M.; Berke, H. *Chem. Commun.* **2010**, *46*, 7981−7983.

(5) (a) Colombo, V.; Galli, S.; Choi, H. J.; Han, G. D.; Maspero, A.; Palmisano, G.; Masciocchic, N.; Long, J. R. *Chem. Sci.* **2011**, *2*, 1311−1319. (b) Low, J. J.; Benin, A. I.; Jakubczak, P.; Abrahamian, J. F.; Faheem, S. A.; Willis, R. R. *J. Am. Chem. Soc.* **2009**, *131*, 15834−15842. (c) Greathouse, J. A.; Allendorf, M. D. *J. Am. Chem. Soc.* **2006**, *128*, 10678−10679.

(6) (a) Bondar, O. A.; Lukashuk, L. V.; Lysenko, A. B.; Krautscheid, H.; Rusanov, E. B.; Chernega, A. N.; Domasevitch, K. V. *CrystEngComm* **2008**, *10*, 1216−1226. (b) Gamez, P.; Mooibroek, T. J.; Teat, S. J.; Reedijk, J. *Acc. Chem. Res.* **2007**, *40*, 435−444.

(7) (a) Zhang, J.-P.; Zhang, Y.-B.; Lin, J.-B.; Chen, X.-M. *Chem. Rev.* **2012**, *112*, 1001−1033. (b) Natarajan, S.; Mahata, P. *Curr. Opin. Solid State Mater. Sci.* **2009**, *13*, 46−53. (c) Aromía, G.; Barriosa, L. A.; Roubeaub, O.; Gamez, P. *Coord. Chem. Rev.* **2011**, *255*, 485−546.

(8) (a) Halcrow, M. A. *Dalton Trans.* **2009**, 2059−2073. (b) Grzywa, M.; Geßner, C.; Denysenko, D.; Bredenkötter, B.; Gschwind, F.; Fromm, K. M.; Nitek, W.; Klemm, E.; Volkmer, D. *Dalton Trans.* **2013**, *42*, 6909−6921. (c) Dincă, M.; Dailly, A.; Liu, Y.; Brown, C. M.; Neumann, D. A.; Long, J. R. *J. Am. Chem. Soc.* **2006**, *128*, 16876−16883. (d) Choi, H. J.; Dincă, M.; Long, J. R. *J. Am. Chem. Soc.* **2008**, *130*, 7848−7850.

(9) (a) Ahmad, M.; Sharma, M. K.; Das, R.; Poddar, P.; Bharadwaj, P. K. *Cryst. Growth Des.* **2012**, *12*, 1571−1578. (b) Xu, Z.; Meng, W.; Li, H.; Hou, H.; Fan, Y. *Inorg. Chem.* **2014**, *53*, 3260−3262. (c) Wang, H.; Zhang, D.; Sun, D.; Chen, Y.; Wang, K.; Ni, Z.-H.; Tianb, L.; Jiang, J. *CrystEngComm* **2010**, *12*, 1096−1102. (d) Liu, Y.; Li, H.; Han, Y.; Lv, X.; Hou, H.; Fan, Y. *Cryst. Growth Des.* **2012**, *12*, 3505−3513.

(10) (a) Zhou, X.-H.; Peng, Y.-H.; Du, X.-D.; Wang, C.-F.; Zuo, J.-L.; You, X.-Z. *Cryst. Growth Des.* **2009**, *9*, 1028−1035. (b) Nicola, C. D.; Karabach, Y. Y.; Kirillov, A. M.; Monari, M.; Pandolfo, L.; Pettinari, C.; Pombeiro, A.J. L. *Inorg. Chem.* **2007**, *46*, 221−230.

(11) (a) Pigge, F. C. *CrystEngComm* **2011**, *13*, 1733−1748. (b) Hawxwell, S. M.; Espallargas, G. M.; Bradshaw, D.; Rosseinsky, M. J.; Prior, T. J.; Florence, A. J.; van de Streek, J.; Brammer, L. *Chem. Commun.* **2007**, 1532−1534.

(12) (a) Tanaka, D.; Nakagawa, K.; Higuchi, M.; Horike, S.; Kubota, Y.; Kobayashi, T. C.; Takata, M.; Kitagawa, S. *Angew. Chem., Int. Ed.* **2008**, *47*, 3914. (b) Trung, T. K.; Trens, P.; Tanchoux, N.; Bourelly, S.; Llewellyn, P. L.; Loera-Serna, S.; Serre, C.; Loiseau, T.; Fajula, F.; Férey, G. *J. Am. Chem. Soc.* **2008**, *130*, 16926−16932.

(13) Burrows, A. D.; Kelly, D. J.; Mahon, M. F.; Raithby, P. R.; Richardson, C.; Stevenson, A. J. *Dalton Tranns.* **2011**, *40*, 5483−5493.

(14) (a) Goswami, A.; Sengupta, S.; Mondal, R. *CrystEngComm* **2012**, *14*, 561−572. (b) Sengupta, S.; Ganguly, S.; Goswami, A.; Bala, S.; Bhattacharya, S.; Mondal, R. *CrystEngComm* **2012**, *14*, 7428−7437. (c) Mondal, R.; Basu, T.; Sadhukhan, D.; Chattopadhyay, T.; Bhunia, M. K. *Cryst. Growth Des.* **2009**, *9*, 1095−1105.

(15) (a) Sengupta, S.; Ganguly, S.; Goswami, A.; Sukul, P. K.; Mondal, R. *CrystEngComm* **2013**, *15*, 8353−8365. (b) Goswami, A.; Bala, S.; Pachfule, P.; Mondal, R. *Cryst. Growth Des.* **2013**, *13*, 5487−5498. (c) Basu, T.; Sparkes, H. A.; Bhunia, M. K.; Mondal, R. *Cryst. Growth Des.* **2009**, *9*, 3488−3496.

(16) Hayter, M.; Bray, D. J.; Clegg, J. K.; Lindoy, L. F. *Synth. Commun.* **2006**, *36*, 707−714.

(17) Sheldrick, G. M. *SHELX97*; University of Göttingen: Göttingen, Germany, 1997.

(18) (a) Sharma, C. V. K.; Zaworotko, M. J. *Chem. Commun.* **1996**, 2655−2656. (b) Miller, P.; Nieuwenhuyzen, M.; Charmant, J. P. H.; James, S. L. *CrystEngComm* **2004**, *6*, 408−412. (c) Lackinger, M.; Griessl, S.; Heckl, W. M.; Hietschold, M.; Flynn, G. W. *Langmuir* **2005**, *21*, 4984−4988.

(19) (a) Dissouky, A.; Mohamad, G. B. *Inorg. Chim. Acta* **1989**, *162*, 263−270. (b) Calahorro, A. J.; Salinas-Castillo, A.; Seco, J. M.; Zuñiga, J.; Colacio, E.; Rodríguez-Diéguez, A. *CrystEngComm* **2013**, *15*, 7636−7639. (c) Konar, S.; Zangrando, E.; Drew, M. G. B.; Ribas, J.; Ray Chaudhuri, N. *Dalton Trans.* **2004**, 260−266. (d) Murrie, M. *Chem. Soc. Rev.* **2010**, *39*, 1986−1995.

(20) (a) Eliel, E. L.; Wilen, S. H. *Stereochemistry of Organic Compounds*, Wiley: Chichester, 1994; p 1000. (b) Sommer, L.; McLick, H. *J. Am. Chem. Soc.* **1969**, *91*, 2001−2010. (c) Goswami, A.; Bala, S.; Pachfule, P.; Mondal, R. *Cryst. Growth Des.* **2013**, *13*, 5487−5498. (d) Bala, S.; Goswami, A.; Sengupta, S.; Ganguly, S.; Bhattacharya, S.; Khanra, S.; Mondal, R. *Cryst. Growth Des.* **2013**, *13*, 5068−5075.